

Supplemental materials

Evolution of Resistance to Phenazine Antibiotics in *Staphylococcus aureus* and its Role During Co-infection with *Pseudomonas aeruginosa*

Tongtong Fu¹, Zhao Cai², Zhuo Yue¹, Hongfen Yang³, Bo Fang⁴, Xinwen Zhang¹, Zheng Fan¹, Xiaolei Pan¹, Fan Yang¹, Yongxin Jin¹, Zhihui Cheng¹, Wuihui Wu¹, Baolin Sun⁴, Robert W. Huigens III³, Liang Yang², Fang Bai^{1*}

¹ State Key Laboratory of Medicinal Chemical Biology, Key Laboratory of Molecular Microbiology and Technology of the Ministry of Education, College of Life Sciences, Nankai University, Tianjin, China.

² School of Medicine, Southern University of Science and Technology (SUSTec), Shenzhen, China.

³ Department of Medicinal Chemistry & Center for Natural Products, Drug Discovery and Development (CNPd3), College of Pharmacy, University of Florida, Gainesville, Florida 32610.

⁴ School of Life Sciences and Medical Center, University of Science and Technology of China, Hefei, Anhui 230027, China.

*, Corresponding authors: Fang Bai (baifang1122@nankai.edu.cn)

This file contains

1) Methods.....	S2-S4
2) Supplementary Table S1-S7.....	S5-S9
3) Supplementary Figure S1-S6.....	S10-S12
4) Reference.....	S12-S13

Methods

Genomic sequencing and reference mapping of HP-22 resistant mutants. Three isolates evolved in MHB only and three HP-22 resistant isolates were first streaked on MHA plates and incubated at 37°C for 16 h. Single colonies were picked and grown in LB at 37°C, 200 rpm for 16 h. Genomic DNA of the *S. aureus* strains was purified using QIAamp DNA Mini Kit (Qiagen, Venlo, The Netherlands) and sequenced on an Illumina (San Diego, CA, USA) MiSeq V3 platform. Nucleotide differences were generated from the CLC Genomics Workbench 8.0 (CLC bio, Aarhus, Denmark). Briefly, adapters and low quality reads were trimmed. Paired-end reads in FASTQ format for HP-resistance and media control (MC) genomes were mapped against the *S. aureus* NCTC8325 genome (NC_007795). The mappings of HPR mutants were compared with the MC isolates, and variants were detected using the quality based variant detection method with the required frequency of 35%.

Quantification of intracellular drug concentration by LC-MS/MS. Overnight cultures of different *S. aureus* strains were diluted into fresh MHB medium and grown to OD₆₀₀=1.0. Around 1×10⁹ CFU of each culture was treated with 0.04 µg/mL (1×MIC), 0.4 µg/mL (10×MIC) of HP-22, and 14 µg/mL (1×MIC) of PYO, respectively, for 30 min. The treated bacterial cells were collected by centrifugation and washed 3 times using phosphate-buffered saline (PBS) to remove extracellular drug residue. In all cases cell pellets were resuspended in PBS. The number of live bacteria (CFU) was determined by serial dilution and plating as previously described¹. Zirconia beads (0.1 mm in diameter) were added to cell pellets for cell breakage by beating. HP-22 was extracted with methanol, PYO was extracted with chloroform:methanol (1:1 v/v), then rotary evaporated to dryness and redissolved in acetonitrile. Drug concentration was determined by a liquid chromatography coupled with an atmospheric pressure chemical ionization-tandem mass spectrometry (APGC-MS/MS, Waters Corporation, UK). An Agilent Zorbax SB-C8 column (2.1 by 30 mm; particle size, 3.5 µm) was used; HP-treated samples were analyzed by the following gradient method using Milli-Q deionized water and acetonitrile mobile phases at a flow rate of 300 µL/min: mobile phase initial conditions were 90:10 water:acetonitrile, which changed to 10:90 at 1 min, then reversed to original conditions at 4 min and held to 5 min when the

equilibrium was reached. The data was acquired by Agilent UHD Q-TOF 6540 system. The mass analysis was performed on the negative ion mode; the MS acquisition parameter used was as follows: capillary voltage 2.5 KV, gas temperature 150°C, drying gas 2.5 L/min and nebulizer 7 bar. PYO-treated samples were analyzed by the following gradient method using Milli-Q deionized water with 0.1% formic acid and acetonitrile mobile phases at a flow rate of 400 μ L/min: mobile phase initial conditions were 80:20 water with 0.1% formic acid:acetonitrile, which changed to 40:60 at 1 min, then reversed to original conditions at 3 min and held to 4 min when the equilibrium was reached. The data was acquired by Agilent UHD Q-TOF 6540 system. The mass analysis was performed on the positive ion mode; the MS acquisition parameter used was as follows: capillary voltage 3.0 KV, gas temperature 300°C, drying gas 2.5 L/min and nebulizer 7 bar. The drug concentration (fg/CFU) was determined by comparing the integrated peak area to a calibration curve, and divided by the corresponding CFU of living cells.

Homology modeling and molecular docking. Homology modeling was conducted in MOE v2015.1001 (Chemical Computing Group Inc.). Template crystal structures were identified through BLAST and downloaded from RCSB Protein Data Bank (PDB ID: 3KKC). The protonation state of the protein and the orientation of the hydrogens were optimized by LigX at the pH of 7 and the temperature of 300 K. First, the target sequence was aligned to the template sequence, and ten independent intermediate models were built. These different homology models were the result of the permutational selection of different loop candidates and side-chain rotamers. Then, the intermediate model which scored best according to the GB/VI scoring function was chosen as the final model, and was subjected to further energy minimization using the AMBER10:EHT force field. The 2D structures of the compound HP-22 was drawn in ChemBioDraw 2014 and converted to 3D structure in MOE through energy minimization. Prior to docking, the force field of AMBER10:EHT and the implicit solvation model of Reaction Field (R-field) were selected. MOE-Dock was used for molecular docking simulations of the HP-22 with TetR21^{WT} and TetR21^{R116C}. The docking workflow followed the “induced fit” protocol, in which the side chains of the receptor pocket were allowed to move according to ligand conformations, with a constraint on their positions. The weight used for tethering side chain atoms to their original positions was 10. For each ligand, all docked poses of which were ranked

by London dG scoring first, then a force field refinement was carried out on the top 20 poses followed by a rescoring of GBVI/WSA dG. The conformations with the lowest free energies of binding were selected as the best (probable) binding modes. Molecular graphics were generated by PyMOL.

Supplementary Tables

Table S1. Common mutations in 3 HPR isolates.

Gene id in <i>S. aureus</i> MW2 (GenBank: BA000033.2)	Gene id in reference genome ^a	Region in reference genome	Mutation	Mutation type	Caused amino acid change ^b	Product
MW0206	SAOUHSC_00192	213558	C > A	SNV	Tyr609>Stop codon	Staphylocoagulase
MW0273	SAOUHSC_00274	292225..292226	GA > AG	MNV	Asp59Ser	Repetitive hypothetical protein
		292228	A > G	SNV	Ile60Val	
		292230..292233	ACCT > GATA	MNV	Ile60Pro61>Met-Ile	
		292237	G > A	SNV	Asp63Asn	
		292241..292242	GC > AT	MNV	Cys64Tyr	
		292246	G > A	SNV	Val66Ile	
		292251..292253	AAA > G	Replacement	Lys68fs	
		292257^292258	- > C	Insertion	Ile70fs	
		292259..292260	TT > GGA	Replacement	Ile70fs	
		292273..292274	TG > -	Deletion	Trp75fs	
		292277	T > A	SNV	Phe76Tyr	
		292280	A > TG	Replacement	Lys77fs	
		292285	T > GC	Replacement	Tyr79fs	
		292288	C > -	Deletion	Arg80fs	
		292291..292293	ATG > TCAA	Replacement	Met81fs	
MW0278	SAOUHSC_00277	293900..293901	GC > AA	MNV	Ser106Lys	Hypothetical protein
MW0517	SAOUHSC_00545	554725	C > A	SNV	Asp1207Glu	Fibrinogen-binding protein SdrD
MW0764	SAOUHSC_00812	794856	A > -	Deletion	Asp624fs	Clumping factor ClfA
		795288	C > A	SNV	Ala768Glu	
MW1681	SAOUHSC_01854	1760735	G > T	SNV	Ala150Glu	Hypothetical protein
MW1742	SAOUHSC_01923	1830624	T > A	SNV	Asn122Ile	Hypothetical protein
MW2297	SAOUHSC_02659	2443574	C > T	SNV	Arg116Cys	TetR21
MW2400	SAOUHSC_02775	2552860	T > G	SNV	Thr58Pro	Hypothetical protein
MW2406	SAOUHSC_02789	2561061..2561062	TT > CC	MNV	Lys164Glu	Hypothetical protein
MW2421	SAOUHSC_02803	2583134	A > C	SNV	Leu413Val	Fibronectin binding protein FnbA
		2583136	T > C	SNV	Asn412Ser	
		2583141	A > T	SNV	Asn410Lys	

^a Reference mapping against the *S. aureus* NCTC 8325 genome (GenBank accession No. NC_007795). ^b SNV, single nucleotide variation; MNV, Multi-nucleotide variation; fs, frame shifting.

Table S2. Susceptibility of *S. aureus* strains to antibiotics and chemical compounds

Antibiotic/chemical	MIC (µg/mL) for <i>S. aureus</i> strains					
	MW2	MW2Δ <i>hprS</i>	MW21 (R116C)	MW21Δ <i>hprS</i>	RN4220	RN21 (R116C)
Chloramphenicol	0.63	0.63	0.63	0.63	1.25	1.25
Ciprofloxacin	0.63	0.63	0.63	0.63	0.63	0.63
Daptomycin	0.63	0.63	0.63	0.63	0.31	0.31
Erythromycin	0.63	0.63	0.63	0.63	0.63	0.63
Linezolid	12.5	12.5	12.5	12.5	6.25	6.25
Ofloxacin	0.39	0.39	0.31	0.39	1.25	1.25
Tetracycline	15.6	15.6	15.6	15.6	0.39	0.39
Vancomycin	0.625	0.625	0.625	0.625	1.25	1.25
Acridavine	15.6	15.6	15.6	15.6	15.6	15.6
Pyocyanin (PYO)	14	14	14	7	14	14
Pyronin Y	3.13	3.13	3.13	3.13	1.56	1.56
Rhodamine 6G	0.98	0.98	0.98	0.98	0.98	0.98
Tetraphenylphosphonium bromide	3.91	3.91	3.91	3.91	3.91	3.91

Table S3. Differential expression analysis by RNA-seq (MRSA MW21 vs wild-type MW2 strain) ^a

Gene ID	Gene Name	Product and description	Regulation	Fold change	P value
MW2296	<i>hprS</i>	hypothetical protein	Up	24.26	6.47E-165
MW2298	<i>corA</i>	divalent cation transporter	Up	1.84	0.00011
MW0770	<i>cspC</i>	cold-shock protein C	Up	1.8	1.27E-05
MW2477		hypothetical protein	Up	1.76	0.000924
MW0779	<i>argO</i>	arginine exporter protein	Up	1.7	0.000241
MW1537	<i>rpsT</i>	30S ribosomal protein S20	Up	1.68	9.77E-05
MW2327	<i>yndB</i>	glutathione S-transferase; activator of Hsp90 ATPase 1 family protein	Up	1.68	0.00204
MW2394	<i>cntK</i>	diaminopimelate epimerase; staphylopine biosynthesis	Up	1.64	0.00448
MW1380	<i>SH3b</i>	peptidoglycan hydrolase	Up	1.63	0.00406
MW1087	<i>pyrF</i>	orotidine 5'-phosphate decarboxylase	Up	1.61	0.0018
MW0837	<i>yabR</i>	nucleotidyltransferase	Up	1.57	0.000541
MW0135	<i>cap8L</i>	capsular polysaccharide synthesis enzyme	Up	1.56	0.000519
MW2392	<i>cntM</i>	staphylopine biosynthesis	Up	1.52	0.017577
MW1450	<i>ypuF</i>	predicted metal-dependent hydrolase	Up	1.51	0.013523
MW2034		bacterial ATP synthase I	Up	1.5	0.010327
MW0706		hypothetical protein	Down	-1.53	0.00655
MW1551		hypothetical protein	Down	-1.53	0.012343
MW0516	<i>sdrC</i>	fibrinogen-binding protein	Down	-1.55	0.013364
MW0553		hypothetical protein	Down	-1.55	0.008342
MW1997		hypothetical protein	Down	-1.55	0.00971
MW0554		hypothetical protein	Down	-1.56	0.003678

MW1980		ketol-acid reductoisomerase	Down	-1.56	0.00617
MW0801		hypothetical protein	Down	-1.57	0.005659
MW1871		hypothetical protein	Down	-1.58	0.007702
MW0517	<i>sdrD</i>	fibrinogen-binding protein	Down	-1.59	0.001413
MW0654		hypothetical protein	Down	-1.62	0.004028
MW2125		hypothetical protein	Down	-1.65	0.004603
MW0552		hypothetical protein	Down	-1.66	0.003412
MW0561		hypothetical protein	Down	-1.69	0.001597
MW0307		hypothetical protein	Down	-1.71	0.002415
MW1325	<i>norB</i>	multidrug efflux MFS transporter	Down	-1.71	7.48E-05
MW0306	<i>ulaA</i>	PTS system ascorbate-specific transporter subunit IIC	Down	-1.72	0.001137
MW2433		hypothetical protein	Down	-1.72	0.000866
MW1150		hypothetical protein	Down	-1.74	0.001719
MW2094		hypothetical protein	Down	-1.76	0.001475
MW0509		hypothetical protein	Down	-1.78	0.000252
MW1057		hypothetical protein	Down	-1.78	0.001168
MW1328		alanine dehydrogenase	Down	-1.79	1.42E-05
MW1349		hypothetical protein	Down	-1.8	0.000907
MW1327		threonine dehydratase	Down	-1.89	5.43E-05
MW2395		hypothetical protein	Down	-1.9	0.000306
MW1039		hypothetical protein	Down	-1.93	0.000118
MW1326		hypothetical protein	Down	-1.95	7.54E-06
MW2402		hypothetical protein	Down	-1.99	2.95E-05
MW2280		hypothetical protein	Down	-2.2	2.86E-09
MW0084	<i>spa</i>	protein A	Down	-2.39	3.66E-07

^a Including the genes that expression level ≥ 1.5 -fold change. Three biological replications of each strain were conducted in RNA-seq experiments.

Table S4. Top 5 identified HprS structural analogs in PDB (bacteria)

Rank ^a	PDB Hit	TM-score ^b	IDEN ^c	Cov ^d	Describes
1	5AYM	0.907	0.107	0.922	MFS iron transporter ferroportin BbFPN of <i>Bdellovibrio bacteriovorus</i>
2	4GBY	0.775	0.057	0.944	MFS glucose transporter XylE of <i>Escherichia coli</i>
3	3O7Q	0.772	0.075	0.882	MFS fucose transporter FucP of <i>E. coli</i>
4	3WDO	0.758	0.084	0.896	MFS drug efflux transporter YajR of <i>E. coli</i>
5	4M64	0.729	0.071	0.922	MFS Na ⁺ /melibiose symporter MelB of <i>Salmonella typhimurium</i>

^a Ranking of proteins is based on TM-score of the structural alignment between the query structure and known structures in the PDB library.

^b TM-score is a measure of global structural similarity between query (HprS) and template protein.

^c IDEN is the percentage sequence identity in the structurally aligned region.

^d Cov represents the coverage of the alignment by TM-align and is equal to the number of structurally aligned residues divided by length of the query protein.

Table S5. Top 5 HprS homologous GO templates in PDB (bacteria)

Rank ^a	Cscore ^{GO}	TM-score	IDEN	Cov	PDB Hit	Describes
1	0.24	0.7724	0.07	0.88	3O7Q	MFS fucose transporter FucP of <i>E. coli</i>
2	0.21	0.6418	0.07	0.92	1PV6A	MFS lactose permease of <i>E. coli</i>
3	0.21	0.6148	0.04	0.82	2GFP	MFS multidrug transporter EmrD of <i>E. coli</i>
4	0.20	0.6452	0.05	0.91	1PW4	MFS glycerol-3-phosphate transporter GlpT of <i>E. coli</i>
5	0.20	0.6243	0.08	0.84	2XUT	MFS oligopeptide transporter of <i>E. coli</i>

^a Ranking of proteins is based on Cscore^{GO} value, which is a combined measure for evaluating global and local similarity between query and template protein. It's range is [0-1] and higher values indicate more confident predictions.

Table S6. Clinical isolates that harboring TetR21^{R116C} (identical protein: WP_000656764.1).

<i>S. aureus</i> strain	NCBI Assembly	Resource and Description
A8115	GCF_000174535.1	Isolated from patients with bloodstream infection who failed or had persistent infection while being treated with daptomycin ² .
A8117	GCF_000175955.1	
21236	GCF_000332665.1	<i>Staphylococcus</i> isolates that aid in determining the genetic basis for drug resistance. This work was supported by the US National Institute of Allergy and Infectious Diseases (NIAID), Genome Sequencing Centers for Infectious Diseases (GSCID) program.
502A	GCF_000597965.1	Bacterial interference in treating staphylococcal disease in newborn babies during the 1960s and early 1970s. However, the practice was abandoned after several infections and a death were attributed to the 502A strain ³ .
ATCC 27217	GCF_002088055.1	
NCTC10804	GCF_900458375.1	
FDAARGOS_14 (NRS149)	GCF_001018775.2	Isolated from nares of nurse. Collected and sequenced by US Food and Drug Administration (FDA) ⁴ .
FDAARGOS_16	GCF_001019355.2	Isolated from clinical samples. Collected and sequenced by FDA.
FDAARGOS_359	GCF_002554295.1	
AW7	GCF_006861725.1	Isolated from a patient with bacteremia in Switzerland in the 1980s and commonly used in treatment and virulence studies ⁵ .

Table S7. Primers used in this study

Name	Sequence (5'-3')	Purpose
pCN51- <i>tetR21</i> -F	GGTCAATGTCTGAACGGTACCTTAATAGACAAATACACCCACATTGTTC	Expression of <i>tetR21</i> in <i>S. aureus</i>
pCN51- <i>tetR21</i> -R	TCCTCTAGAGTCGACCTGCAGTTAAGTTAGTGAATCAAGGTTTGATTATG	
pCN51- <i>hprS</i> -F	CAGGTCGACTCTAGACTGCAGAAATATTCAACACATTGTCTAATAAGGAGG	Expression of <i>hprS</i> in <i>S. aureus</i>
pCN51- <i>hprS</i> -R	AGAATAGGCGCGCCTCTGCAGTTATGACGGCACTTCAGTACGTTT	
pCN51- <i>corA</i> -F	GGTCAATGTCTGAACCTGCAGGTAATACTCGCTTTTCCTAAATCCTTT	Expression of <i>corA</i> in <i>S. aureus</i>
pCN51- <i>corA</i> -R	TCCTCTAGAGTCGACCTGCAGTTATAATTTCTGTTTACGCCATAAGAAA	
<i>tetR21</i> -LIC-F	CAGGGCGCCATGAAAGAAGATAGGCGAATTAG	LIC cloning
<i>tetR21</i> -LIC-R	GACCCGACGCGGTTAAGTTAGTGAATCAAGGTTTG	
<i>tetO</i> -F	TTGTGTTATTGAACAATGTGG	SPR/EMSA
<i>tetO</i> -R	GTGTTGAATATTTTCGCATGTTGTC	SPR/EMSA

half <i>tetO</i> -F	GTGTATTGTTTATTCCAC	SPR
<i>RtetR21</i> -UP-F- <i>EcoRI</i>	CACTCATCGCAGTGCAGCGGAATTCATCACCCATACCAGTTAACACAGCT	<i>tetR21</i> point mutation
<i>RtetR21</i> -UP-R	TGTAAGTAAATGTCCCTCTATTGATATCAGCGCTGTTGTTATGTC	
<i>RtetR21</i> -DN-F	GACATAACAACACGCGCTGATATCAATAGAGGGACATTTTACTTACA	
<i>RtetR21</i> -DN-R- <i>Sall</i>	AAGCTTGCATGCCTGCAGGTCGACTTCTGTTGTTTCGATGGCTTGG	
<i>RhprS</i> -UP-F- <i>EcoRI</i>	CACTCATCGCAGTGCAGCGGAATTCACAGACATATCTCGCAATCCAGC	<i>hprS</i> deletion
<i>RhprS</i> -UP-R	AGCAACTATGATTATCTTGGCTGTATCAAGTTTAGTTTCAGCT	
<i>RhprS</i> -DN-F	AGCTGAAACTAACTTGATACAGCCAAGATAATCATAGTTGCT	
<i>RhprS</i> -DN-R- <i>Sall</i>	AAGCTTGCATGCCTGCAGGTCGACATCCATGACGCTGTATGATCTAATGG T	
<i>RcorA</i> -UP-F- <i>EcoRI</i>	CACTCATCGCAGTGCAGCGGAATTCAGACAAATACACCCACATTGTTC	<i>corA</i> deletion
<i>RcorA</i> -UP-R	TGGTCATCAATTGGCAACGGCACCATGACGCTGTATGATCTAATGGTGT	
<i>RcorA</i> -DN-F	ACACCATTAGATCATAACGCGTCATGGTGCCGTTGCCAATTGATGACCA	
<i>RcorA</i> -DN-R- <i>Sall</i>	AAGCTTGCATGCCTGCAGGTCGACATGCTTGATAGCAGCTTATATCTTAGC	
pOS1- <i>hprS</i> -PF	CAAAGCCTTAAAGACGATCCGGGGAATTCCTCTAAATTATCATGAATATG TTGGA	<i>lacZ</i> promoter assay
pOS1- <i>hprS</i> -PR	TCCCAGTCACGACGTTGTAAAACGACGGGATCCGGAAATATATTCATTTTA TTAATTACCTCCTTATTAGAC	<i>lacZ</i> promoter assay
pOS1- <i>tetR21</i> -PF	CAAAGCCTTAAAGACGATCCGGGGAATTCCTCATAGCATCTTTTGAAAAGT C	<i>lacZ</i> promoter assay
pOS1- <i>tetR21</i> -PF	TCCCAGTCACGACGTTGTAAAACGACGGGATCCGGTCGCCTATCTTCTTT CAAAAATAAATCAACCT	<i>lacZ</i> promoter assay
Q- <i>tetR21</i> -F1	CAATTGGAACGCACGAGTCA	qRT-PCR
Q- <i>tetR21</i> -R1	TACATCTCTGGAACGCCTCC	
Q- <i>hprS</i> -F	CGTCGTGCAACATCGTATCA	qRT-PCR
Q- <i>hprS</i> -R	TAAGGCCACGAAACCAAGA	
Q- <i>corA</i> -F	AGTAGAACCAGACCGAGAAGA	qRT-PCR
Q- <i>corA</i> -R	TCAGCGTCACAACTGTTACG	
Q- <i>tet38</i> -F	ATGAATGTTGAATATTCTAA	qRT-PCR
Q- <i>tet38</i> -R	TGGCTACAGAAATCAAT	
Q- <i>lmrS</i> -F	CAGTATAAATCAATGGTCTA	qRT-PCR
Q- <i>lmrS</i> -R	CTTTATCTGCCTTGTTATCA	
Q-16S-F1	ACAAAGTGACAGGTGGTGCA	qRT-PCR
Q-16S-R1	GTTTGTCAACCGGCAGTCAAC	

Supplementary Figures

Figure S1

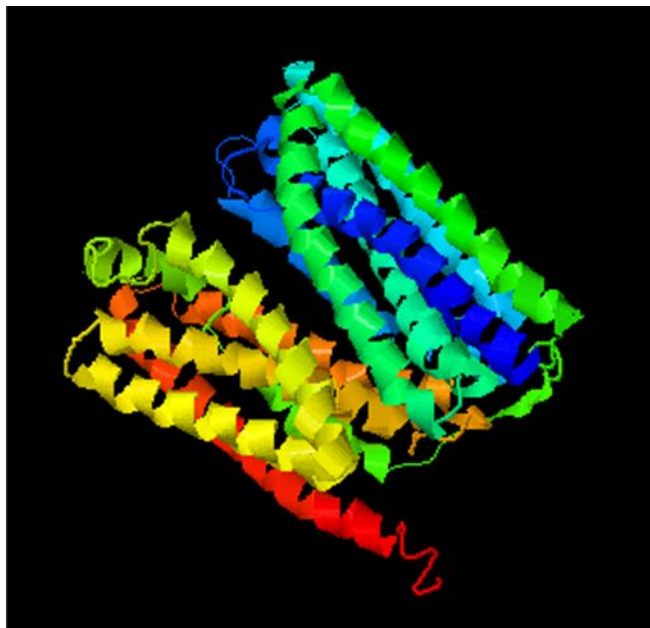


Figure S1. 3D structural model₁ of HprS generated by I-TASSER⁶⁻⁷. C-score=-1.36; Estimated TM-score = 0.55±0.15; Estimated RMSD = 10.1±4.6Å.

Figure S2

Name	Sites			p-value
LmrA_Bt	GAATCAAGAT	AATAGACCAGTCAC	TATATTTTGTG	4.25e-8
QacR_Sa	TTATAATCCT	TATAGACCGATCGC	ACGGTCTATA	2.48e-7
TetR21_tet38	TGGTTAGACA	AATAGACAAATCAC	TATACAAATA	7.33e-7
MtrR_Ng	GCCCTCGTCA	AACCGACCCGAAAC	GAAAACGCCA	1.96e-6
AcrR_E.coli	GTCAAAAGTT	AATAAACCCATTGC	TGCGTTTATA	2.11e-6
* TetR21_MW2296	TACATATTAT	AATAGACAACATGC	GAAATATTCA	3.30e-6
EthR_Mtb	ATGTCGACAC	TATCGACACGTAGT	AAGCTGCCAG	6.28e-6

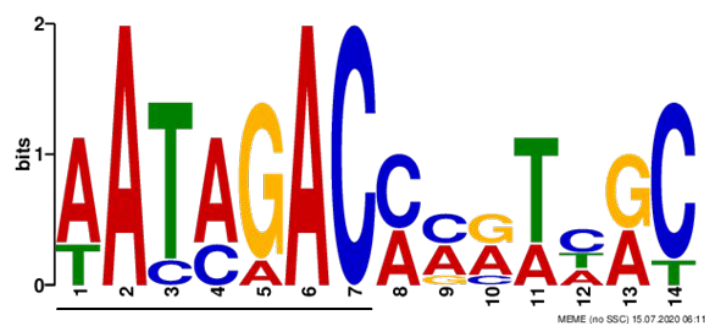


Figure S2. Identification of the potential TetR21 binding motif by MEME⁸. The conserved sequences of binding sites are shown in color. TetR family repressor binding sequences

including: LmrA of *Bacillus subtilis*, QacR of *Staphylococcus aureus*; *tet38* promoter region of *S. aureus* MW2; MtrR of *Neisseria gonorrhoeae*; AcrR of *Escherichia coli*; EthR of *Mycobacterium tuberculosis*. The asterisk indicates the intergenic region between MW2296 and *tetR21* in *S. aureus* MW2. The motif consensus was “AATAGACMMRTHRC”, in particular the underlined “AATAGAC” motif showed strictly conserved.

Figure S3

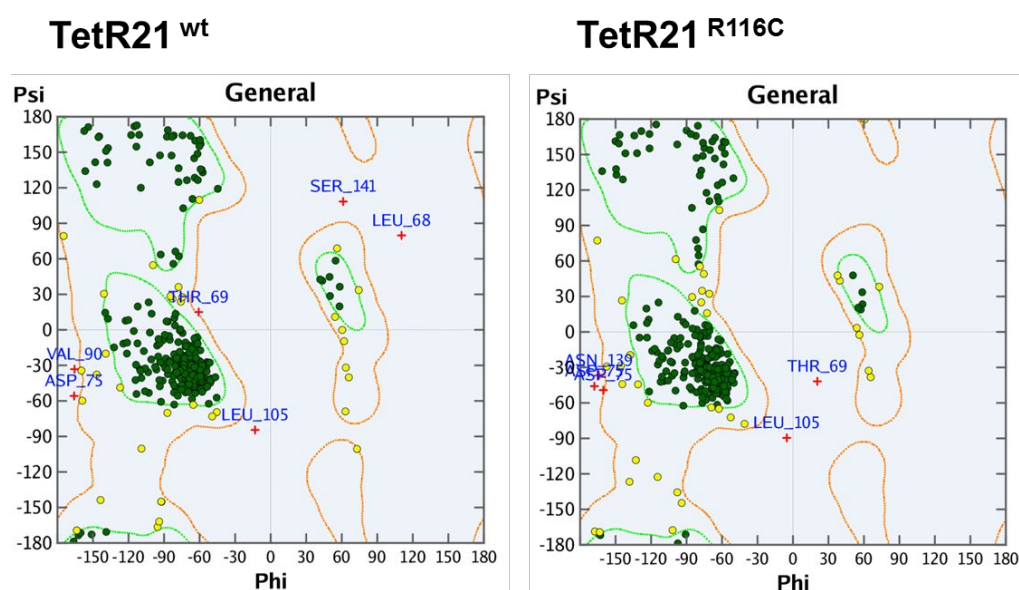


Figure S3. Ramachandran plot for TetR21 proteins in homology modeling. Dark green dots represent the residues in favored regions; yellow dots represent the residues in allowed regions; red dots represent the residues in irrational regions.

Figure S4

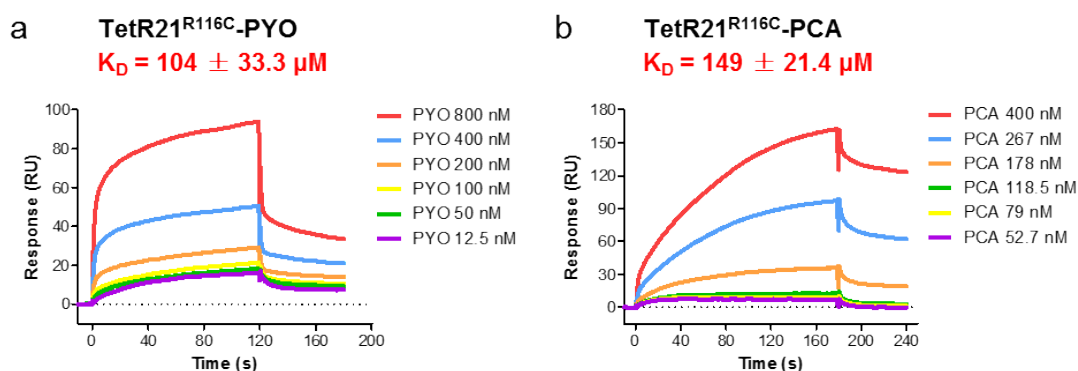


Figure S4 Surface Plasmon Resonance (SPR) analyses of binding of natural phenazines to TetR21^{R116C}. (a) Interactions between pyocyanin (PYO) and TetR21^{R116C}. (b) Interactions between phenazine-1-carboxylic acid (PCA) and TetR21^{R116C}.

Figure S5

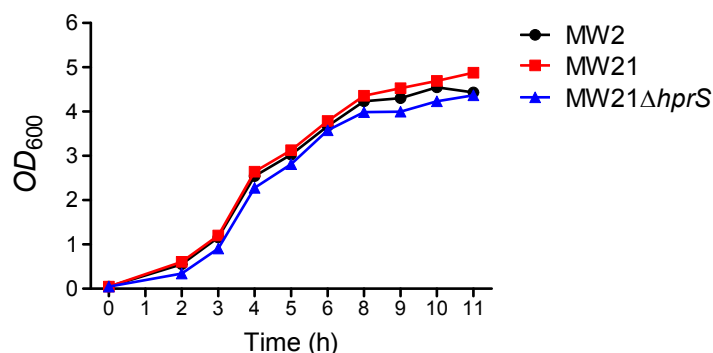


Figure S5 Growth curves of *S. aureus* strains.

Figure S6

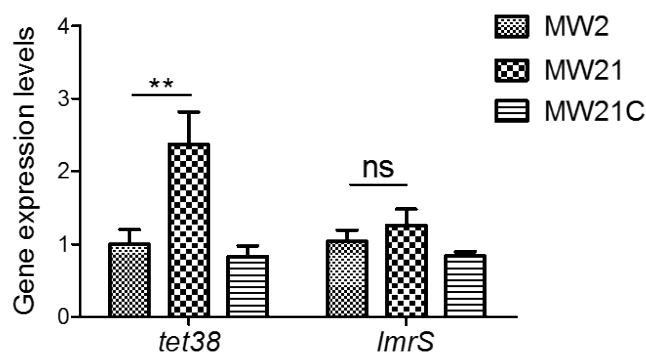


Figure S6 Quantitative PCR determination of the expression levels of *tet38* and *lmrS* genes in wild-type MRSA MW2, MW2 containing point mutation R116C in *tetR21* (MW21), and MW21 carrying the complementary plasmid pCN51-*tetR21* (MW21C). **, $P < 0.01$, ns, non-significant.

Reference

- (1). Xiaolei, P.; Yuanyuan, D.; Zheng, F.; Chang, L.; Bin, X.; Jing, S.; Fang, B.; Yongxin, J.; Zhihui, C.; Shouguang, J., In vivo host environment alters *Pseudomonas aeruginosa* susceptibility to aminoglycoside antibiotics. *Front Cell Infect Microbiol.* **2017**, *7*, 83.
- (2). Peleg, A. Y.; Miyakis, S.; Ward, D. V.; Earl, A. M.; Rubio, A.; Cameron, D. R.; Pillai, S.; Moellering, R. C., Jr.; Eliopoulos, G. M., Whole genome characterization of the mechanisms of daptomycin resistance in clinical and laboratory derived isolates of *Staphylococcus aureus*. *PloS One.* **2012**, *7* (1), e28316.
- (3). Houck, P. W.; Nelson, J. D.; Kay, J. L., Fatal septicemia due to *Staphylococcus aureus* 502A. Report of a case and review of the infectious complications of bacterial interference programs. *Am J Dis Child.* **1972**, *123* (1), 45-8.
- (4). Cafiso, V.; Bertuccio, T.; Spina, D.; Purrello, S.; Campanile, F.; Di Pietro, C.; Purrello, M.; Stefani, S., Modulating activity of vancomycin and daptomycin on the expression of autolysis cell-wall turnover and membrane charge genes in hVISA and VISA strains. *PloS One.* **2012**, *7* (1), e29573.
- (5). Cameron, D. R.; Ramette, A.; Prazak, J.; Entenza, J.; Haenggi, M.; Que, Y. A.; Resch, G., Draft Genome Sequence of Methicillin-Resistant *Staphylococcus aureus* Strain AW7, Isolated from a Patient with Bacteremia.

Microbiol Resour Announc. **2019**, 8 (40), e00806-19.

(6). Zhang, Y., I-TASSER server for protein 3D structure prediction. *BMC bioinformatics.* **2008**, 9, 40.

(7). Roy, A.; Kucukural, A.; Zhang, Y., I-TASSER: a unified platform for automated protein structure and function prediction. *Nat Protoc.* **2010**, 5 (4), 725-38.

(8). Bailey, T. L.; Elkan, C., Fitting a mixture model by expectation maximization to discover motifs in biopolymers. *Proceedings. Proc Int Conf Intell Syst Mol Biol.* **1994**, 2, 28-36.